ALKBH5 regulates chicken adipogenesis by mediating *LCAT* mRNA stability depending on m^{6}A modification

Xiaohuan Chao[1,3], Lijin Guo[1,2], Chutian Ye[1,2], Aijun Liu[1,2], Xiaomeng Wang[1,2], Mao Ye[1,2], Zhexia Fan[1,2], Kang Luan[1,2], Jiahao Chen[3], Chunlei Zhang[3], Manqing Liu[1,2], Bo Zhou[3], Xiquan Zhang[1,2], Zhenhui Li[1,2]* and Qingbin Luo[1,2]*

Abstract

Background Previous studies have demonstrated the role of N6-methyladenosine (m^{6}A) RNA methylation in various biological processes, our research is the first to elucidate its specific impact on *LCAT* mRNA stability and adipogenesis in poultry.

Results The 6 100-day-old female chickens were categorized into high (*n* = 3) and low-fat chickens (*n* = 3) based on their abdominal fat ratios, and their abdominal fat tissues were processed for MeRIP-seq and RNA-seq. An integrated analysis of MeRIP-seq and RNA-seq omics data revealed 16 differentially expressed genes associated with to differential m^{6}A modifications. Among them, *ELOVL* fatty acid elongase 2 (*ELOVL2*), pyruvate dehydrogenase kinase 4 (*PDK4*), fatty acid binding protein 9 (*PMP2*), fatty acid binding protein 1 (*FABP1*), lysosomal associated membrane protein 3 (*LAMP3*), lecithin-cholesterol acyltransferase (*LCAT*) and solute carrier family 2 member 1 (*SLC2A1*) have ever been reported to be associated with adipogenesis. Interestingly, *LCAT* was down-regulated and expressed along with decreased levels of mRNA methylation methylation in the low-fat group. Mechanistically, the highly expressed *ALKBH5* gene regulates *LCAT* RNA demethylation and affects *LCAT* mRNA stability. In addition, *LCAT* inhibits preadipocyte proliferation and promotes preadipocyte differentiation, and plays a key role in adipogenesis.

Conclusions In conclusion, *ALKBH5* mediates RNA stability of *LCAT* through demethylation and affects chicken adipogenesis. This study provides a theoretical basis for further understanding of RNA methylation regulation in chicken adipogenesis.

Keywords MeRIP-seq, Chicken, Adipogenesis, *ALKBH5*, *LCAT*, Stability

*Correspondence:
Zhenhui Li
lizhenhui@scau.edu.cn
Qingbin Luo
qbluo@scau.edu.cn
[1]State Key Laboratory of Livestock and Poultry Breeding, South China Agricultural University, Guangzhou, China
[2]College of Animal Science, South China Agricultural University, Guangzhou, China
[3]College of Animal Science and Technology, Nanjing Agricultural University, Nanjing, China

Chao *et al. BMC Genomics*   (2024) 25:634

Page 2 of 14

Background

Adipose tissue is widely regarded as the major site of lipid deposition and lipid metabolism. Adipose tissue has energy storage, endocrine and metabolic functions, it affects the health, metabolic balance and immune homeostasis in humans and animals [1–5]. A number of metabolic diseases caused by obesity have become an increasing global health problem [6, 7]. Similarly, excessive deposition of abdominal fat in chickens can also lead to metabolic diseases and increase feed wastage in poultry, adding enormously to the cost of poultry production.

Adipogenesis is a complex process with transcription factors at the core, coordinated with epigenetic factors and transcriptional cofactors together to form a complex and programmed transcriptional regulatory network [8–10]. Epigenetic modification plays an important role in fat formation and deposition [11–14]. In addition to DNA methylation and histone modification, RNA methylation has been implicated in the regulation of adipogenesis [15–18]. In 3T3L1 cells, *Zfp217* is involved in the regulation of overall m6A modification by activating the transcription of the m6A demethylase *FTO*. This suggests that *Zfp217* plays an important role in the generation and differentiation of fat [19]. Similarly, studies conducted b demonstrated that *FTO* enhances RNA stability in chicken preadipocytes in an m6A-dependent manner, thereby increasing *CTNNB1* expression. Furthermore, m6A has been demonstrated to promote the translation of HIF1A mRNA and to regulate the browning and thermogenesis of white fat cells [20]. However the mechanism of *LCAT* mRNA methylation on abdominal adipogenesis in poultry is unclear.

The MeRIP-seq technique employs m6A-specific antibodies to enrich M6A-modified RNA fragments, thereby facilitating the analysis of m6A modifications and RNA epigenetic modifications within the transcriptome range [21]. We aim to identify the mRNA of interest by MeRIP-seq to further explore the regulatory mechanism of m6A methylation in chicken adipogenesis. This study is the first to clarify the role of *LCAT* m6A methylation during adipogenesis. Lecithin cholesterol acyltransferase (*LCAT*) is a key protein in the peripheral high-density lipoprotein metabolism pathway, which has been reported to be mainly involved in cholesterol reverse transport and energy metabolism [22–24]. To date, *LCAT* plays an important role in atherosclerosis and is associated with abdominal subcutaneous fat and abdominal visceral fat [25–28]. We observed that both *LCAT* expression and its mRNA methylation were downregulated in adipose tissue in the low-fat group. *ALKBH5*, an m6A demethylase, was found to regulate mRNA fate through m6A demethylation and has been implicated in the biological regulation of several cancers [29, 30]. *ALKBH5* has been reported to affect transcription and translation by regulating mRNA fate through m6A demethylation [31, 32]. *ALKBH5* has been demonstrated to be involved in the pathogenesis of osteoarthritis by influencing the stability of *CYP1B1* mRNA through m6A demethylation [33]. Furthermore, studies have demonstrated that *ALKBH5* regulates the energy metabolism of haematopoietic stem cells and progenitors through RNA stability, which is mediated by m6A modification [34]. In addition, studies have shown that *ALKBH5* is associated with obesity and can regulate the proliferation and differentiation of chicken adipocyte progenitors [35, 36]. Using qPCR, we found that *ALKBH5* was differentially expressed between the high-fat group and the low-fat groups. To our knowledge, no study has shown how *ALKBH5* mediates LCAT demethylation to influence adipogenesis in chickens. The purpose of this study was to investigate the potential m6A modification sites using sequencing data and impact of *LCAT* mRNA demethylation on chicken adipogenesis by cell biology. This can help to enhance our understanding of the regulatory mechanism of RNA methylation in chicken adipogenesis.

Methods

Animal testing and ethical statements

The animals provided by Guangdong Wens for this study were six female Sanhuang chickens, and the single cage feeding was carried out after the growing stage, and pellets were fed twice a day. At 100 days of age, they were euthanised by dislocation of the first cervical vertebra, and their abdominal fat tissues were collected, weighed and stored in liquid nitrogen. The body weights and abdominal fat weights of the 6 experimental animals are listed in Table 1. The animal experiments were approved by the Animal Care Committee of South China Agricultural University (SCAU#2,017,015; September 13, 2017).

MeRIP-seq and mRNA-seq

The 6 adipose tissues were divided into high-fat (HF) and low-fat (LF) groups based on their abdominal fat ratio. Total RNA was extracted from the fat tissues and DNA was removed using Dnase I. Then the rRNA was removed. The RNA was then chopped into small

Table 1 Abdominal fat percentage of 6 subjects

Sample	weight (g)	Abdominal fat weight (g)	Abdominal fat rate (%)
L1	1576.2	61.8	3.92
L2	1550	56.8	3.66
L3	1360	50.3	3.70
Mean±SD	1495.4±68.12	56.3±3.33**	3.76±0.08**
H1	1701.5	133.8	7.86
H2	1750.1	135.8	7.76
H3	1596.9	122.6	7.68
Mean±SD	1682.83±45.20	130.73±4.11	7.77±0.05

fragments, added to antibodies for binding and enriched for m⁶A. The IP library and input library were constructed and MeRIP-seq and mRNA-seq were performed using the Hiseq platform, which was then complemented by E-GENE technology.

Cell culture and cell transfection

Immortalised chicken preadipocyte 1 (ICP-1) was provided by the Li Hui laboratory of Northeast Agricultural University (Heilongjiang, China) [37, 38]. ICP-1 was cultured in a mixed medium of DMEM and DMEM/ F_{12} (Gibco, CA, United States) with 15% fetal bovine serum (Gibco, CA, United States) and 1% streptomycin/penicillin (Invitrogen, CA, United States) at 37 °C with 5% CO_2. Lipofectamine 3000 (Invitrogen, CA, United States) was used for cell transfection. According to the manufacturer's instructions, the transfection dose of plasmids or oligonucleotides for different plates was as follows 14–28 μg for each 10 cm plate, and 1 μg/well or 50 nM/well for 12-well plates.

Total RNA extraction

Total RNA extraction from cells and tissues was performed using TriQuick Reagent (SolarBio, Beijing, China) according to manufacturer's instructions. A total of 50 mg of homogenised tissue or 10^6 cells were lysed by adding 1 mL of TriQuick Reagent (SolarBio, Beijing, China) at room temperature. 200 μL chloroform (Damao, Tianjin, China) was added, mixed, allowed to stand at room temperature for 2–3 min and centrifuged at 12,000 × g at 4 ℃ for 15 min. The upper aqueous phase was transferred to a new 1.5 mL centrifuge tube. Next, 500 μL isopropanol (Damao, Tianjin, China) was added to the tube, left at room temperature for 10 min to precipitate the RNA, centrifuged at 12,000 × g at 4 ℃ for 10 min, the supernatant was discarded, and 1 mL 75% ethanol (Damao, Tianjin, China). The mixture was centrifuged at 12,000×g at 4 ℃ for 10 min and the supernatant was discarded. Then, 1 mL of 75% ethanol was added to the tube (Damao, Tianjin, China) and centrifuged at 12,000 × g at 4 ℃ for 2 min. Finally, 25 μL of RNase-free water was added to the tubes to the dissolve RNA (SolarBio, Beijing, China), and stored at -80℃.

Plasmids construction and oligonucleotides synthesis

The complete CDS sequence of *ALKBH5* (XM_004945197.4) was synthesised by TSINGKE (Beijing, China) and subcloned into the Nhe I and Hind III sites of the pcDNA3.1-Flag vector (Promega, WI, United States). And the complete CDS sequence of *LCAT*

Table 2 The sequence information of oligonucleotide

Fragment name	Fragment sequences (5' to 3')
si-*LCAT*	CCTGGCGTCAGGTGATAAT

(NM_001293094.2) was subcloned into the Hind III and BamH I sites of pcDNA3.1 vector (Promega, WI, United States) by TSINGKE (Beijing, China). The plasmids were named as *ALKBH5* and *LCAT*-pcDNA3.1. In addition, siRNA of *LCAT* was synthesized by RioBio (Guangdong, China), and the sequence of the oligonucleotides is listed in Table 2.

Flow cytometry analysis

After 48 h of transfection, the cells were digested with 0.25%-EDTA trypsin (Gibco, CA, United States). After washing with PBS, the cells were immobilised in 75% pre-cooled ethanol. The fixative was removed, and the cells were washed with PBS. Finally, 0.5 mL of propidium iodide (PI) solution (Beyotime, Shanghai, China) was added and the cell pellet was gently resuspended. The cells were incubated at 37℃ for 30 min without light. Cells were analysed using a CytoFlex instrument (Beckman, CA, United States).

Oil red O staining

After 6 h of transfection, preadipocyte differentiation was induced using a medium containing 15% fetal bovine serum and 0.2% oleic acid (Sigma, CA, United States). After 48 h of induction, the cells were washed with PBS and fixed with 300 μL of 4% paraformaldehyde for 30 min at room temperature. The cells were washed twice with PBS, 300 μL of Oil Red O Staining Solution (SolarBio, Beijing, China) was added and incubated at room temperature for 1 h. The staining solution was then removed and the cells were washed four times with PBS. The stained cells were observed and photographed under an electron microscope (Nikon, Tokyo, Japan). Finally, 300 μL of isopropyl alcohol was used to clean the stained cells and absorbance values were determined at 510 nm (biorad, CA, United States).

MeRIP-qPCR

The Magna MeRIP™ m⁶A (MeRIP) Kit (Magna, United States) was used to detect m⁶A methylation in cells according to the manufacturer's protocol. 300 μg of RNA was fragmented using RNA Fragmentation Buffer at 94 °C for 5 min. End fragmentation with the addition of 0.5 M EDTA. Then 3 M sodium acetate, glycogen (100 μg/mL) and anhydrous ethanol were added, mixed and incubated at -80 ℃ overnight. The samples were then centrifuged at 15,000 × g for 25 min at 4 ℃, the supernatant was discarded, 1 mL of 75% ethanol was added and centrifuged at 15,000 × g for 15 min at 4 ℃. Finally add 300 μL of RNase-free water and store at -80 °C. Take 25 μL of Magnetic Beads A/G Blend and add 10 μL to each tube. m⁶A antibody or normal mouse IgG antibody was incubated for 30 min at room temperature, adsorbed on a magnetic rack and the supernatant was discarded. 10

Chao *et al. BMC Genomics*   (2024) 25:634

Page 4 of 14

μL of fragmented RNA was taken as input, the remaining RNA was added to RNase inhibitor and IP buffer 5×, and finally RNASe-free water was added to l mL. 500 μL was added to the immunoprecipitation-loaded magnetic beads, incubated at 4 ℃ for 2 h, washed twice with IP buffer, eluent added to each tube, and eluted twice at 4 ℃ for 1 h each time. Finally, RNA was purified and the purified RNA was used for reverse transcription and RT-qPCR.

m⁶A dot blot

The m⁶A Dot Blot was used to detect the total RNA methylation level in the cells. After 48 h of transfection, total RNA from ICP-1 cells was harvested and 1 μg RNA was denatured at 95 ℃ for 3 min. The denatured RNA was cross-linked to a positively and negatively charged nylon membrane. The unbound RNA was then washed with TBST for 5 min. After blocking with 5% skimmed milk for 1 h, the membrane was incubated with anti-m⁶A (1 : 500; ab151230, abcam), and anti-mouse IgG antibodies (1 : 5,000; ab190475, abcam) at 4 °C overnight. The membrane is not cut prior to hybridisation with the antibody. Finally, Odyssey Instrument (Li-cor, CA, United States) and ImageJ Software were used for visual analysis and grey scale analysis of the membrane.

RNA binding protein immunoprecipitation (RIP)

After 48 h of transfection, the RNA-Binding Protein Immunoprecipitation kit (Magan, United States) was used to detect the binding between *LCAT* mRNA and *ALKBH5* in cells. The RIP assay was performed according to the manufacturer's protocol for RNA-Binding Protein Immunoprecipitation (Magan, United States).

Reverse transcription and real-time quantitative PCR (qPCR)

Reverse transcription PCR for mRNA was performed using MonScriptTM RTlll All-in-one Mix (Monad, Wuhan, China) according to the manufacturer's protocol. ChamQ Universal SYBR qPCR Master Mix (Vazyme, Nanjing, China) and ABI QuantStudio 5 (Thermo Fisher, NY, United States) were used for real-time fluorescence quantification. NCBI Primer Design was used to design qPCR primers, and primer information is provided in Supplementary file 1 Table S1. The mRNA of *GAPDH* was used as an internal control.

Prediction of methylation sites of m⁶A

According to the methylation modification sites given by the sequencing results, the m⁶A methylation sites of *LCAT* were predicted using http://genome.ucsc.edu/. The sequence of the predicted sites is shown in Supplementary file 1 Table S2. According to the predicted results, the primers for qPCR were designed using Premier

Primer 5.0 software and the primer sequences are shown in Supplementary file 1 Table S3.

Actinomycin D treatment

ALKBH5 was overexpressed in ICP cells and treated with Actinomycin D 24 h later. 5 μg/well Actinomycin D was added to a 12-well plate. Cells were harvested at 0 h, 3 h and 6 h and *LCAT* expression levels were determined at different time points.

Western blotting

Proteins were extracted from cells after 48 h of transfection using ice-cold radio immunoprecipitation (RIPA) lysis buffer containing 1 mM phenylmethyl sulfonyl fluoride (Beyotime, Shanghai, China). Protein samples were separated on a 12% SDS-PAGE gel (EpiZyme, Shanghai, China) run at 120 V for 60 min. The proteins were transferred to polyvinylidene fluoride (PVDF) membrane (Bio-Rad, CA, United States). After blocking with 5% skim milk for 1 h and the membrane is sheared at 38 kDa. The membrane was incubated with anti-PPARγ (1 : 1,000; bs-0530R, BIOSS), ALKBH5 (1 : 1,000; 49,015, CST), LCAT (1 : 1,000; CQA2612; CohesionBio) and anti-GAPDH (1 : 2,000; bsm-33,033 M, BIOSS) antibodies at 4 °C overnight. Anti-rabbit IgG HRP-antibody (1 : 10,000; 7074P2, CST) was used as secondary antibody. Finally, the protein bands were visualised using Odyssey (Li-COR, CA, USA) and the grey value (image density) was measured using ImageJ software. Alternatively, the film can be exposed by inserting it into an X-ray clamp.

Data statistics and analysis

Student's t-test was used to compare the differences between groups. Each group had at least three between-group replicates. All experimental data are expressed as mean±SEM. ∗$P < 0.05$; ∗∗$P < 0.01$; ns: no significant.

Results

MeRIP-seq analysis of m⁶A methylation in High-Fat Group and Low-Fat Group

From an epigenetic perspective, the aim of this study was to investigate the regulatory mechanism of RNA methylation in chicken fat deposition. Abdominal adipose tissues from 3 high-fat (HF) and 3 low-fat (LF) broilers were selected for MeRIP-seq. Quality control results indicated that the percentage of Q30 (base detection accuracy≥99.9%) was greater than 97% (Supplementary file 1 Table S4). In addition, at least 17,008 peaks were obtained for each sample (Supplementary file 1 Table S5). All raw data were submitted to the NCBI SRA database. |Fold Change| ≥ 2, and P-value<0.05 were set as differential screening criteria, a total of 979 differential m⁶A methylation modification sites were obtained by performing MeRIP-seq in abdominal fat RNA. The most common

motif type was RRACH, and the three motifs with the most significant differences were GGACA, GAACU and AAACU (Fig. 1A). The distribution of peaks in gene elements with significant differences was statistically analysed and it was found that most of the peaks were located in distal intergenic regions (Fig. 1B). Among the differential m6A methylation modification sites, 76 were up-regulated and 903 were down-regulated (Fig. 1C). The results of GO function analysis of genes associated with differential m6A methylation modification sites showed that these genes could be enriched in cell differentiation, nucleus and ATP binding, glucose transmembrane transport, growth and glucose transmembrane transport

activity (Fig. 1D). KEGG pathway enrichment analysis showed that these genes may be enriched in the PPAR signalling pathway, adipokine signalling pathway, fatty acid elongation and FOXO signalling pathway, suggesting that these genes may be involved in chicken adipogenesis (Fig. 1E). The top 20 abundant m6A methylation modification sites are listed in Table 3, including *LOC396477*, *C11H16ORF87*, and *CDCA9*. Through GO and KEGG analysis, some differential m6A methylation modifier genes (*LCAT, PDK4, PRMT7, SIRT6, SLC2A1* and *SIRT5*), which may be related to lipid metabolism, were considered as potential candidates in the subsequent study [39–41].
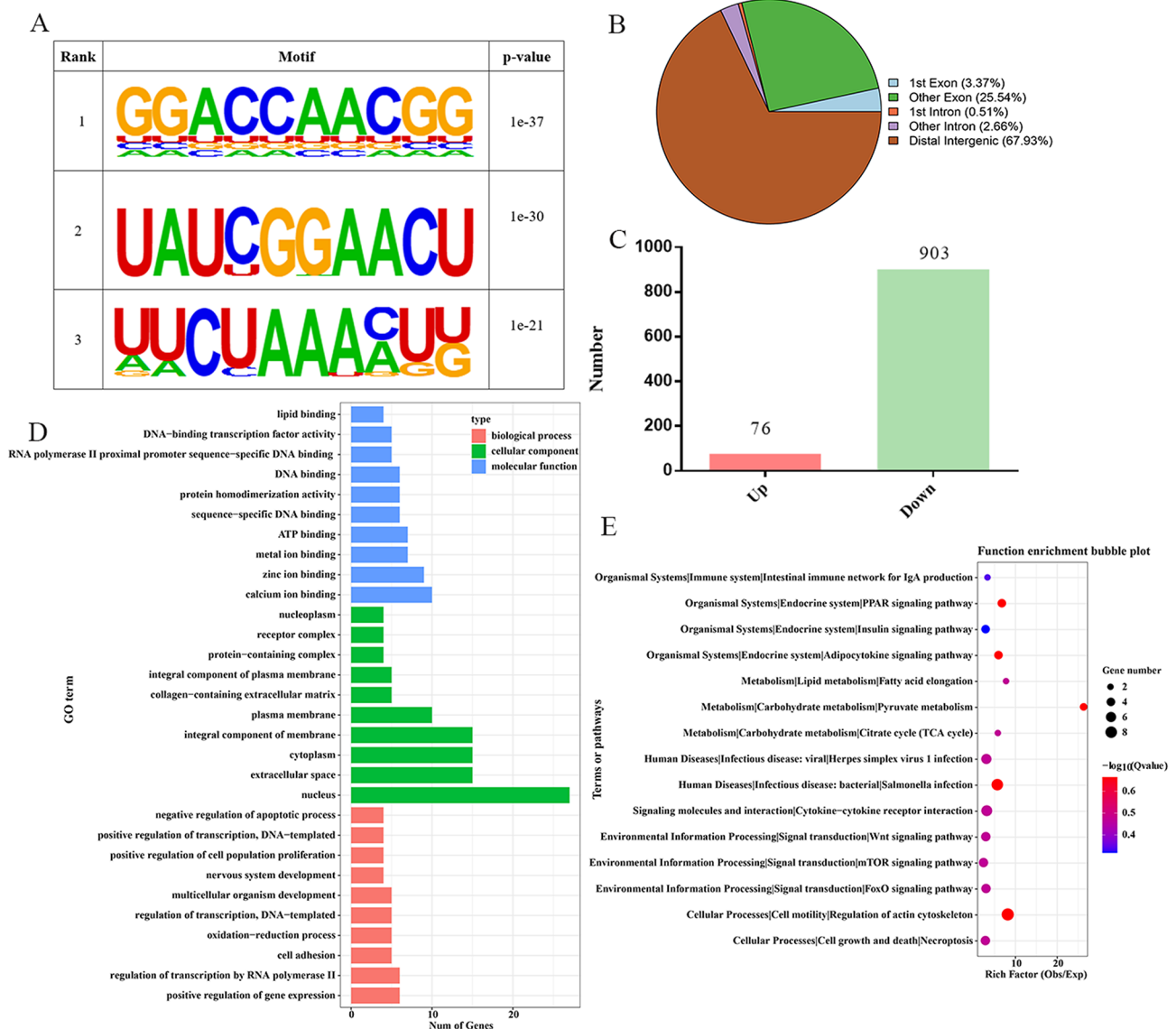

Fig. 1 Analysis of MeRIP-seq in chicken abdominal fat tissues between he high-fat and low-fat groups. **(A)** The regional distribution of difference m6A methylation modification enrichment. **(B)** Markedly different motif types. **(C)** Statistical analysis of the number of different m6A modification sites in the high-fat group and the low-fat group. **(D)** Genes associated with difference m6A methylation modification sites enriched GO term. X axis: gene number; Y axis: GO terms. **(E)** Genes associated with difference m6A methylation modification sites enriched KEGG pathways. X axis: rich factor; Y axis: pathway

Chao *et al. BMC Genomics*   (2024) 25:634

Page 6 of 14

Table 3 The top 20 abundant mRNA with differences in m^{6}A methylation modification sites

Chrom	PeakStart	PeakEnd	mRNA	Foldchange	Regulation
chr30	1500775	1504141	*LOC396477*	429	Up
chr11	7757976	7758485	*C11H16ORF87*	66.6	Up
chr11	7757976	7766226	*C11H16ORF87*	65.1	Up
chr11	7757926	7758496	*CDCA9*	56.3	Up
chr7	12131545	12132291	*FZD5*	45	Up
chr25	3853425	3854692	*CRP*	43.3	Up
chr19	7780459	7782595	*TBX4*	39	Up
chr23	2823327	2824045	*SRRM1*	34.2	Up
chr5	38323050	38324277	*ACYP1*	212	Down
chrZ	7906219	7906869	*ENHO*	148	Down
chr1	1.96E+08	1.96E+08	*ART7B*	103	Down
chr2	1.21E+08	1.21E+08	*STMN2*	82.5	Down
chr13	2400602	2401232	*PCDHGC3*	78.1	Down
chr19	3576183	3577516	*P2RX1*	77.4	Down
chr9	3926622	3927368	*CEP63*	75.9	Down
chr7	28520894	28521342	*C7H2ORF76*	57.7	Down
chr27	7209722	7210406	*RARA*	55.8	Down
chr18	806620	807041	*MYOCD*	55.8	Down
chr30	389347	389704	*HUC*	55.8	Down
chr23	5630172	5631159	*PPT1*	35.2	Down
chr13	11172623	11175401	*ARL10*	32.5	Down

Genome-wide mRNA screening and analysis identified mRNA Associated with Fat Deposition

To explore the regulatory mechanism of abdominal fat deposition in chickens, mRNA sequencing was performed on the same samples and submitted to the NCBI SRA database. For RNA-seq, |Fold Change| ≥ 2, and P-value<0.05 were considered as screening criteria for differentially expressed genes (DEGs). A total of 273 DEGs were obtained (Fig. 2A). Among them, 195 genes were up-regulated and 78 genes were down-regulated in the high-fat group (Fig. 2C). GO functional analysis showed that these DEGs could be enriched in glucose transmembrane transport, glucose transmembrane transporter activity, fatty acid metabolism, and lipid binding (Fig. 2B, D). Some genes related to fat deposition were identified by GO and KEGG analysis, suggesting that these genes might be involved in abdominal adipogenesis in chickens, including *SLC2A2, PMP2, SLC2A1, HNF4A, FABP7, PDK4* and *LCAT* (Table 4) [42–44].

Combined analysis of MeRIP-seq and mRNA-seq Indicated that mRNA methylation of *LCAT* may regulate fat deposition

To further understand the relationship between m^{6}A methylation modification and mRNA expression in abdominal fat deposition, we performed association analysis on the omics data of MeRIP-seq and mRNA-seq. A total of 16 DEGs were found to be associated with differential m^{6}A methylation modifications, suggesting

that these m^{6}A methylation modifications may regulate their mRNA expression (Fig. 3A). KEGG enrichment analysis of these 16 genes showed that these genes were most significantly enriched in the lipid metabolism pathway (Fig. 3B), among which the adipose-related genes were *ELOVL2, PDK4, PMP2, FABP1, LAMP3, LCAT* and *SLC2A1* (Table 5) [45–47]. Combined with MeRIP-seq and mRNA-seq, it was found that *LCAT* mRNA level was positively correlated with the reduction of its mRNA methylation level, indicating that *LCAT* mRNA stability may be responsible for adipogenesis in chickens.

ALKBH5, as a demethylase, mediated the degradation of *LCAT* and affect its stability

ALKBH5 is differentially expressed in chicken abdominal adipose tissue between HF and LF groups, prompting an investigation into its role in demethylation and its functional impact on chicken abdominal adipose tissue(Fig. 4A, B and C). We constructed an *ALKBH5* overexpression vector and qPCR results showed that *LCAT* expression was significantly downregulated when *ALKBH5* was overexpressed (Fig. 4D). This suggests that *ALKBH5* affects the expression of *LCAT*. This was followed by MeRIP-qPCR to confirm that the m^{6}A sites were present on *LCAT* mRNA. Compared to the IgG group, IP production using the m^{6}A specific antibody showed an enrichment of *LCAT* mRNA, which was consistent with the sequencing results (Fig. 4E). To further investigate the effect of *ALKBH5* on *LCAT* of preadipocytes, we overexpressed *ALKBH5* on ICP, and Dot Blot showed that ALKBH5 down-regulated the total RNA methylation level of preadipocytes compared to the blank group (Fig. 4F). Meanwhile, MeRIP-qPCR was used to confirm *ALKBH5* mediated *LCAT* mRNA demethylation upon *ALKBH5* overexpression, and *LCAT* mRNA enrichment was reduced in the *ALKBH5* group compared to the control (Fig. 4G). RIP was used to further investigate whether LCAT binds AKLBH5, and the results showed that *LCAT* mRNA was enriched in the ALKBH5 group compared to the IgG group. AKLBH5 protein was shown to be bound to *LCAT* mRNA (Fig. 4H). In addition, ALKBH5 overexpressing preadipocytes were treated with ActinomycinD, and qPCR results showed that ALKBH5 continuously down-regulated the expression of *LCAT* at different treatment times compared with the blank group. At the same time, *ALKBH5* down-regulated the expression of *LCAT* at the same treatment time (Fig. 4I). In conclusion, the Dot Blot results demonstrated that *ALKBH5* could down-regulate the methylation level of ICP cells in a global manner. Subsequently, MeRIP-qPCR and RIP experiments demonstrated that *ALKBH5* binds to the methylation modification site on *LCAT* mRNA, and that *ALKBH5* further influenced the stability of *LCAT* following treatment with actinomycin D.
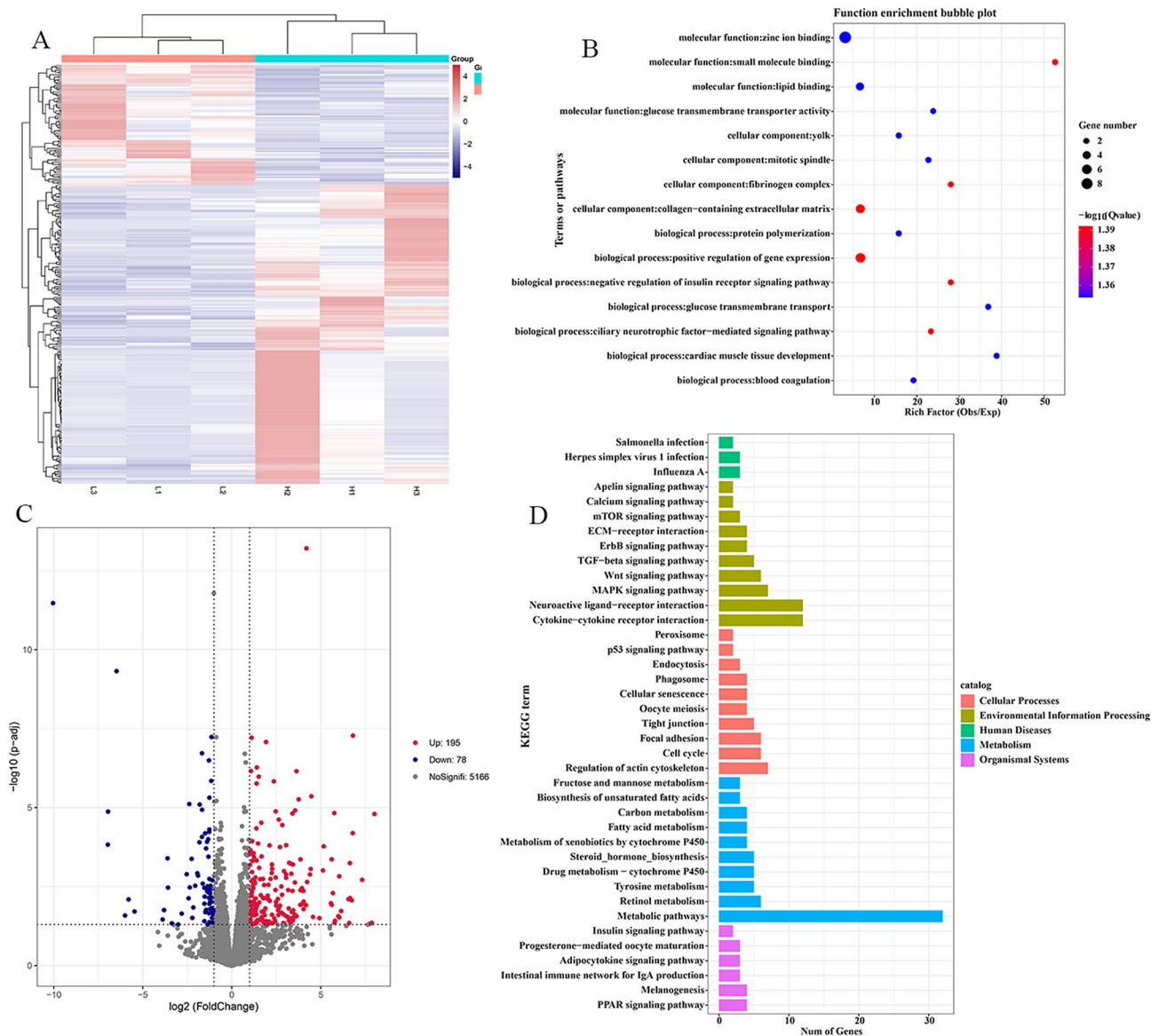
Fig. 2 Analysis of mRNA differentially expressed in chicken abdominal fat tissues between the high-fat and low-fat groups. (**A**, **C**) Heat map and Volcano plot for low-fat_VS_high-fat DEGs. (**B**) The GO function enrichment analysis for DEGs. (**D**) The KEGG pathways classification analysis for DEGs.

Table 4 Differentially expressed mrnas associated with fat formation and lipid metabolism

Gene name	Low-Fat Expression	High-Fat Expression	log2Ratio (HF/LF)	*P* value	Up Down	Gene description
HNF4A	0	47.98	8.020987199	1.58E-05	Up	hepatocyte nuclear factor 4 alpha
SLC2A2	4.35	133.34	4.93083747	0.031024063	Up	facilitated glucose transporter
PMP2	9.9	116.91	3.558754643	1.23E-05	Up	fatty acid binding protein 9
FABP1	15.18	137.28	3.179519135	0.003994144	Up	Fat body protein 1
ELOVL6	223.13	973.74	2.125485279	0.00015671	Up	ELOVL fatty acid elongase 6
FABP7	115.85	348.89	1.590417855	0.001824541	Up	fatty acid binding protein 7
INSIG1	973.75	1982.43	1.025331849	0.000645623	Up	insulin induced gene 1
SLC2A1	1105.01	504.49	-1.131247985	5.76E-08	Down	facilitated glucose transporter
PDK4	15911.74	7564.62	-1.07276	0.022237047	Down	pyruvate dehydrogenase kinase 4
LCAT	273.63	717.75	1.390884877	0.044774122	Up	lecithin-cholesterol acyltransferase

Chao *et al. BMC Genomics*   (2024) 25:634
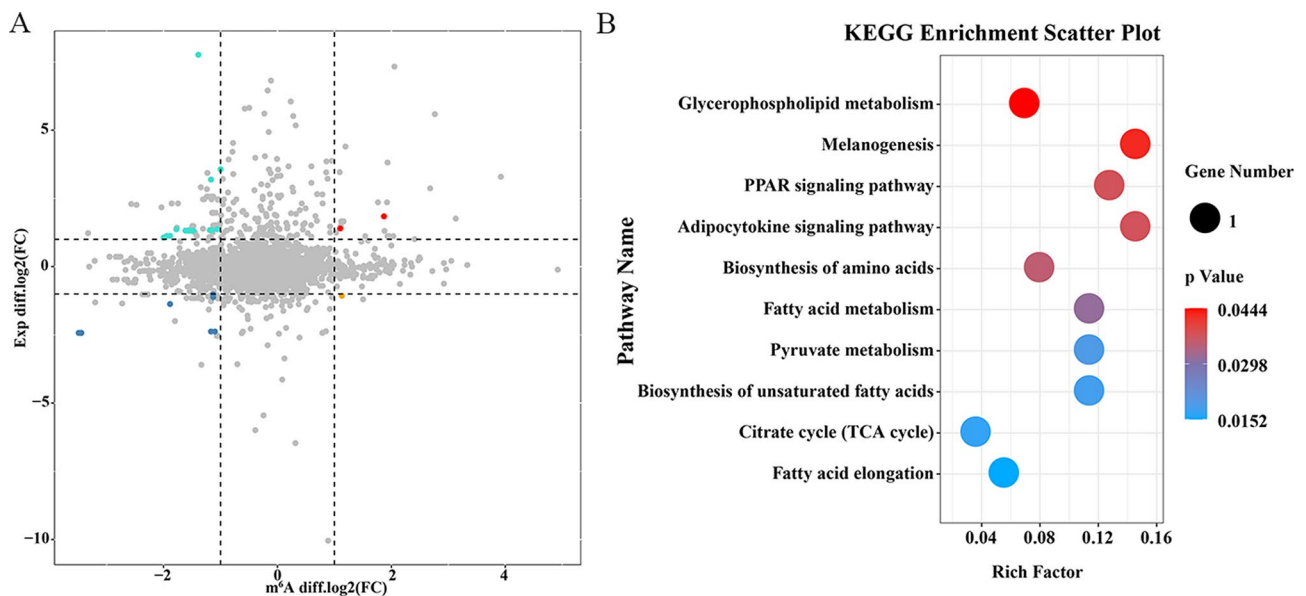
Page 8 of 14

Fig. 3 Combined analysis of MeRIP-seq and mRNA-seq. **(A)** Four quadrants between differential m⁶A methylation modification associated genes and differential expression genes. **(B)** The KEGG pathways enrichment analysis for differential m⁶A methylation modification associated genes and differential expression genes

Table 5 Differential m⁶A modification and DEGs associated with lipid metabolism

Chrom	PeakStart	PeakEnd	mRNA	Foldchange	Regulation
chr2	62916247	62916723	*ELOVL2*	10.7	Down
chr2	23907156	23907546	*PDK4*	7.74	Up
chr2	1.21E+08	1.21E+08	*PMP2*	27.9	Down
chr4	86132634	86135786	*FABP1*	2.72	Down
chr9	16523508	16524286	*LAMP3*	10.5	Down
chr11	1035168	1036088	*LCAT*	12.5	Up
chr21	6462015	6462525	*SLC2A1*	10.7	Down
chr33	6174474	6190421	*PC*	6.37	Down

LCAT inhibits the proliferation of preadipocyte

The qPCR and western blot results showed that *LCAT* was differentially expressed in adipose tissue between HF and LF, which was consistent with the sequencing data (Fig. 5A, B and C). To further explore the role of *LCAT* during fat deposition in chickens, we continued the study of cellular function. We constructed the plasmid and siRNA to overexpress or knock down *LCAT* (Fig. 5D). Flow cytometry results showed that the preadipocyte cycle stagnated in G1 phase after *LCAT* overexpression, leading to a decreased proportion of S phase cells (Fig. 5E and Supplementary file 2 Fig S1). Meanwhile, the qPCR results showed that *LCAT* overexpression up-regulated the expression of *PCNA*, *Cyclin D1*, *Cyclin D2* and *Cyclin B2* (Fig. 5F). On the contrary, *LCAT* knockdown promoted their expression (Fig. 5G). It is speculated that *LCAT* suppresses preadipocyte proliferation.

LCAT Promotes differentiation of preadipocyte through PPARγ pathway

We further explored the role of *LCAT* in preadipocyte differentiation. First, oleic acid was used to induce preadipocyte differentiation. The results of qPCR showed that *LCAT* expression increased significantly after differentiation induction (Fig. 6A). Meanwhile, Oil Red O staining showed that *LCAT* promoted the formation of lipid droplets during the differentiation of preadipocytes compared with the blank group (Fig. 6B, D). In contrast, *LCAT* knockdown inhibited lipid droplet formation (Fig. 6C, G). In addition, *LCAT* overexpression promoted the mRNA expression of *LPL* and *PPARγ*, which are considered to be the key preadipocyte differentiation genes in the PPARγ pathway. It also promoted the expression of *ADIPO* and *C/EBPβ* (Fig. 6E, F). The protein levels of PPARγ were increased after *LCAT* overexpression in preadipocytes, whereas *LCTA* knockdown decreased the protein expression (Fig. 6H - K). Taken together, these results suggest that *LCAT* overexpression may accelerate preadipocyte differentiation by promoting the activation of the PPARγ pathway.

Discussion

In poultry, abdominal adipogenesis causes a number of metabolic diseases and feed wastage. Recent studies have shown that m⁶A methylation is involved in the regulation of adipogenesis and plays an important role in the process of adipogenic differentiation [48, 49]. Unlike previous studies focusing on m⁶A methylation in mammalian systems, our research provides the first evidence of m⁶A's

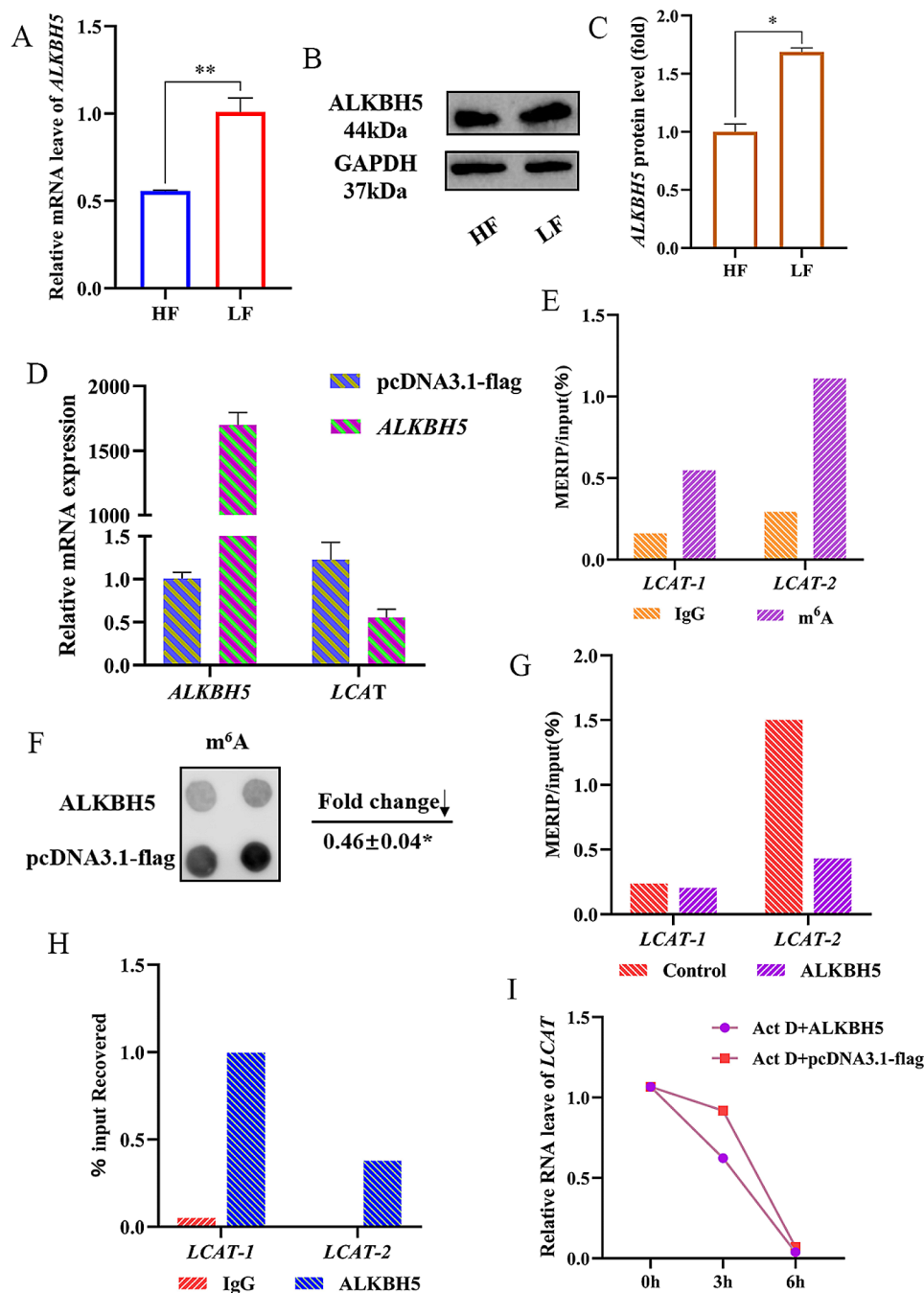Chao *et al. BMC Genomics*   (2024) 25:634

Page 9 of 14

Fig. 4 ALKBH5 mediates LCAT stabilization through demethylation. **(A)** Relative expression of *ALKBH5* in high-fat chicken and low-fat chicken. (**B**, **C**) The western blot for *ALKBH5* protein in HF and LF, full-length blots are presented in Supplementary file 3 B. **(D)** Transfection efficiency of *ALKBH5* and relative expression of *LCAT*. **(E)** The methylation modification sites of LCAT were detected by MeRIP-qPCR. **(F)** m⁶A Dot Blot was used to detect the overall RNA methylation of ICP-1 cells after transfection with *ALKBH5*, full-length blots are presented in Supplementary file 3 A. **(G)** Methylation of *LCAT* mRNA after *ALKBH5* overexpression was detected by MeRIP-qPCR. (H) ALKBH5 protein was detected to bind to RNA of *LCAT* by RIP. **(I)** After transfection of *ALKBH5*, cells were treated with 5 μg/mL Actinomycin D to detect the relative expression of *LCAT*. Data presented as mean ± SEM, *$P < 0.05$; **$P < 0.01$; ns: no significance

role in regulating *LCAT* mRNA stability and adipogenesis in chickens. Our findings suggest that m⁶A methylation is a critical regulatory mechanism in avian species, with potential implications for understanding and manipulating fat metabolism across different organisms. In this

study, we used the sequencing technology to identify a differential gene (*LCAT*) and its mRNA with potential m⁶A modification sites that were significantly associated with abdominal fat deposition. As an m⁶A demethylase, ALKBH5 is involved in a variety of biological regulation
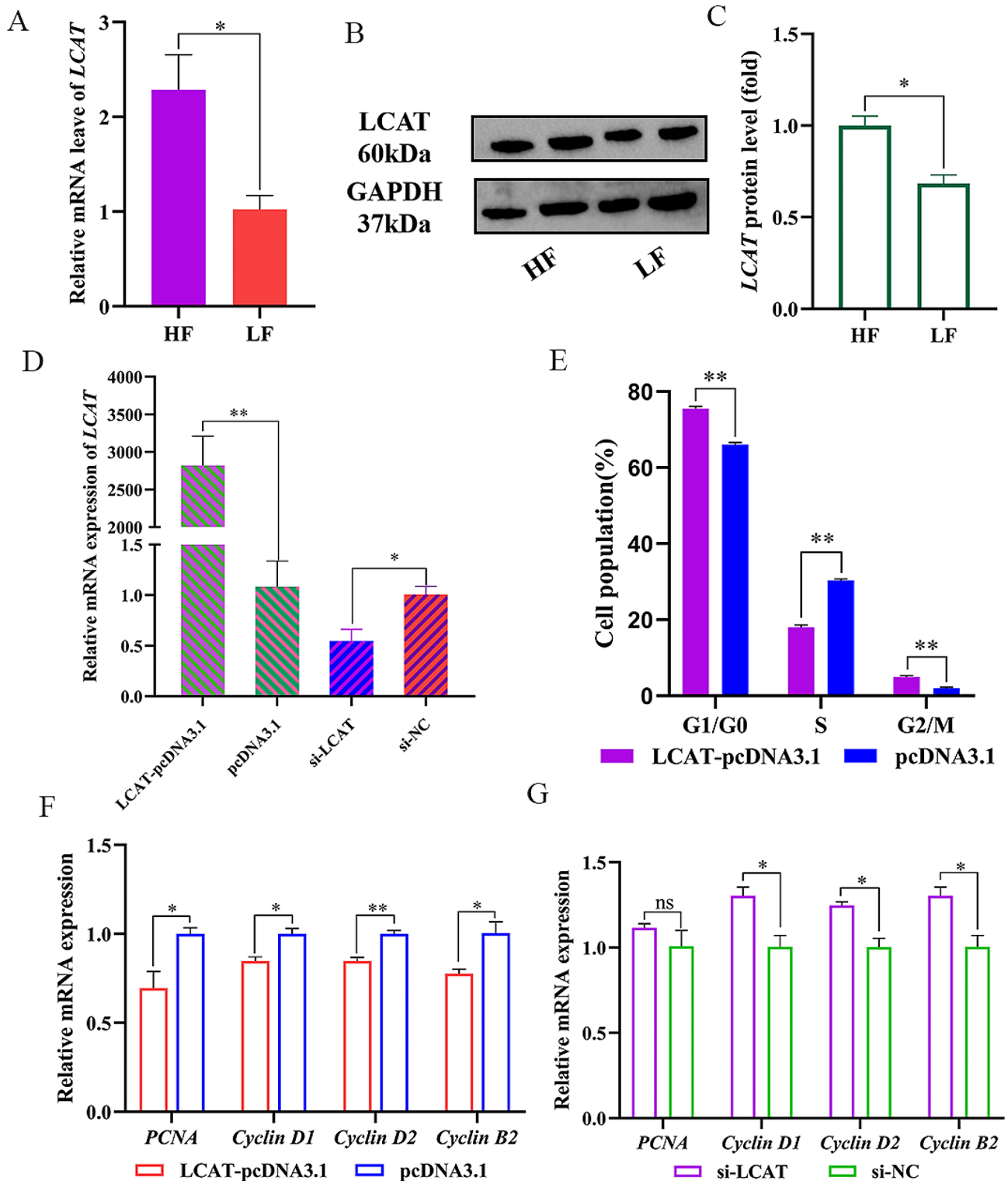
Fig. 5 *LCAT* inhibits the proliferation of preadipocyte. **(A)** Relative expression of LCAT in high-fat chicken and low-fat chicken. (**B**, **C**) The western blot for *LCAT* protein in HF and LF, full-length blots are presented in Supplementary file 3 C. **(D)** Transfection efficiency of *LCAT* and si-*LCAT*. **(E)** Flow cytometry for cell cycle detection of ICP-1 cells. (**F**, **G**) Relative mRNA expression of PCNA, Cyclin D1, ,Cyclin D2, and Cyclin B2 in ICP-1 cells. Data presented as mean ± SEM, *$P < 0.05$; **$P < 0.01$;ns: no significance

Fig. 6 *LCAT* promotes preadipocytes differentiation via PPARγ pathway. **(A)** Relative expression of *LCAT* before and after preadipocytes differentiation. (**B**, **C**) Oil red staining for lipid droplet formation. (**D**, **G**) Lipid droplets change (**E**, **F**) Relative mRNA expression of *LPL*, *ADIPO*, *C/EBPβ*, and *PPARγ* in ICP-1 cells. (**H** - **K**) The western blot for *PPARγ* protein in ICP-1 cells, full-length blots are presented in Supplementary file 3 D. Data presented as mean ± SEM, *P < 0.05; **P < 0.01; ns: no significance

and controls RNA fate in an m[6]A dependent manner [50, 51]. In the previous experiment, we found that ALKBH5 was highly expressed in the low-fat group. Based on the sequencing data, we designed a series of molecular and cellular experiments to explore the demethylation of ALKBH5 on LCAT and the role of *LCAT* in fat deposition. Our results showed that ALKBH5 could regulate the RNA methylation of *LCAT*, affect the stability and promote *LCAT* mRNA. We also found that *LCAT* inhibited the proliferation and promoted differentiation of preadipocytes.

Various transcripts, such as mRNA, lncRNA, and circRNA, have m[6]A methylation modification, which can affect the stability and post-transcriptional processing of RNA [52, 53]. The m[6]A methylation sites in the coding sequence regions (CDS) play an important role in the stability of mRNA [54]. Zhao et al. found that FTO controls the exon splicing of the lipid-forming regulator RUNX1T1 by regulating the level of m[6]a modification

around the splicing site in the CDS regions, to regulate the differentiation [55]. The study by Zhang et al. shows that *METTL3* can regulate mRNA translation through methylation of the CDs region of *LDHA* [56]. Our sequencing data showed that the m[6]A methylation modification site of *LCAT* was located in the CDS region, and the degree of m[6]A methylation modification was greater in the high-fat group than that in the low-fat group. To determine whether *ALKBH5* regulates *LCAT* expression through means of m[6]A dependence. The qPCR, MeRIP-qPCR, RIP and Actinomycin D treatments were used in the chicken preadipocyte model. The results showed that the demethylation of *ALKBH5* accelerated the degradation of *LCAT* mRNA, indicating that the mRNA methylation in the CDS region of *LCAT* enhanced its stability. Studies have shown that m[6]A's regulatory factors are linked to fat [36, 57]. Overexpression of *ALKBH5* increases *FABP5* expression in a m[6]A-*IGF2BP2* dependent manner, leading to lipid metabolism disorders
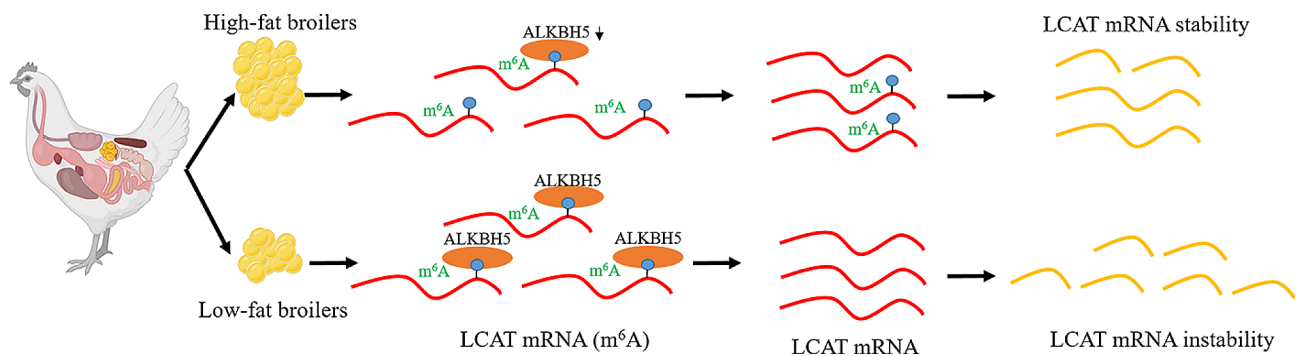
Fig. 7 Schematic diagram of the role of RNA methylation modification of *LCAT* mRNA in abdominal fat deposition in chickens.*ALKBH5* affects the stability of *LCAT* mRNA through demethylation modification, and *LCAT* affects the proliferation and differentiation of ICP cells

[58].The research report that inhibition of *ALKBH5* could promote m^6A modification of *CCL28* mRNA and increase its stability [59]. The regulatory mechanism is the same as for this experiment.

LCAT has been extensively studied in atherosclerosis over the last few decades [22, 25, 60]. However, little is known about its role in fat deposition. Studies have shown that *LCAT* deficiency provides specific protection against diet-induced obesity and insulin resistance by regulating white adipose tissue formation and brown fat cell allocation [61]. Based on the evidence that *LCAT* may be involved in adipose tissue deposition, we further investigated its role in this biological function. Xepapadaki reported that loss of *APOAL* or *LCAT* in mice led to increased sensitivity to body weight, and *LCAT* deficiency resulted in a synergistic reduction in oxidative phosphorylation and non-shivering thermoproduction in white adipose tissue [62]. The expression of *LCAT* has been found to be up-regulated in the treatment of obese people [63]. These data are consistent with our results. In this experiment, *LCAT* expression level was less in the high-fat group. In chicken proadipocytes, flow cytometry showed that *LCAT* inhibited the G1 to S phase transition, and qPCR showed that *LCAT* inhibited the expression of cell cycli-related genes. Meanwhile, *LCAT* promoted the PPARγ signalling pathway at the protein and RNA levels, and the effects of *LCAT* overexpression and interference on preadipocyte differentiation were determined by qPCR and Oil red O staining. However, the research by Nesan et al. showed that *LCAT* deficiency could promote the differentiation of cholesterol-dependent satellite cells into brown adipocytes [24]. This is contrary to our results, and the reasons for this difference are unclear. Due to the limited size of the sequencing sample employed in this experiment, it is possible that certain limitations may be encountered. In order to validate our findings and improve the generality of the results, larger and more diverse studies will be conducted in the future.

Conclusions

In summary, our results indicate that *LCAT* expression and the degree of m^6A methylation modification were down-regulated in the low-fat group. In addition, we demonstrated the relationship between *ALKBH5* and *LCAT*, and confirmed that *ALKBH5* affects the stability of *LCAT* mRNA through demethylation (Fig. 7). Whereas *LCAT* inhibits preadipocyte formation and promotes differentiation. This study identified, *ALKBH5* was identified to be involved in adipogenesis by demethylation mediating *LCAT* mRNA stability. It is expected to provide evidence for the role of RNA methylation in fat process.

Supplementary Information

The online version contains supplementary material available at https://doi.org/10.1186/s12864-024-10537-2.

Supplementary Material 1

Supplementary Material 2

Supplementary Material 3

Declarations

Animal testing and Ethics approval
This study was carried out in compliance with the ARRIVE guidelines 2.0 (https://arriveguidelines.org/). All methods were carried out in accordance with relevant guidelines and regulations. Animals in animal experiments are euthanized and approved by the Animal Care Committee of South China Agricultural University (SCAU#2017015; September 13, 2017).

Consent for publication
Not applicable.

Competing interests
The authors declare no competing interests.

References
1. Kershaw EE, Flier JS. Adipose tissue as an endocrine organ. J Clin Endocrinol Metab. 2004;89:2548–56. https://doi.org/10.1210/jc.2004-0395.
2. Alpert MA, Omran J, Bostick BP. Effects of obesity on Cardiovascular Hemodynamics, Cardiac morphology, and ventricular function. Curr Obes Rep. 2016;5:424–34. https://doi.org/10.1007/s13679-016-0235-6.
3. van Baak MA, Mariman ECM. Mechanisms of weight regain after weight loss - the role of adipose tissue. Nat Rev Endocrinol. 2019;15:274–87. https://doi.org/10.1038/s41574-018-0148-4.
4. White U, Ravussin E. Dynamics of adipose tissue turnover in human metabolic health and disease. Diabetologia. 2019;62:17–23. https://doi.org/10.1007/s00125-018-4732-x.
5. Lin H, et al. Secretion of miRNA-326-3p by senescent adipose exacerbates myocardial metabolism in diabetic mice. J Transl Med. 2022;20:278. https://doi.org/10.1186/s12967-022-03484-7.
6. Landrier JF, Derghal A, Mounien L. MicroRNAs in obesity and related metabolic disorders. Cells. 2019;8. https://doi.org/10.3390/cells8080859.
7. Sanchez-Ceinos J, et al. Impaired mRNA splicing and proteostasis in preadipocytes in obesity-related metabolic disease. Elife. 2021;10. https://doi.org/10.7554/eLife.65996.
8. Hong J, Li S, Wang X, Mei C, Zan L. Study of expression analysis of SIRT4 and the coordinate regulation of bovine adipocyte differentiation by SIRT4 and its transcription factors. Biosci Rep. 2018;38. https://doi.org/10.1042/BSR20181705.
9. Wang W et al. A PRDM16-Driven Metabolic Signal from Adipocytes Regulates Precursor Cell Fate. *Cell Metab* 30, 174–189 e175, https://doi.org/10.1016/j.cmet.2019.05.005 (2019).
10. Yu K, et al. Activating transcription factor 4 regulates adipocyte differentiation via altering the coordinate expression of CCATT/enhancer binding protein beta and peroxisome proliferator-activated receptor gamma. FEBS J. 2014;281:2399–409. https://doi.org/10.1111/febs.12792.
11. Chen Y, et al. The novel long noncoding RNA lncRNA-Adi regulates adipogenesis. Stem Cells Transl Med. 2020;9:1053–67. https://doi.org/10.1002/sctm.19-0438.
12. Jiang R, et al. circRNA profiling reveals an abundant circFUT10 that promotes adipocyte proliferation and inhibits adipocyte differentiation via sponging let-7. Mol Ther Nucleic Acids. 2020;20:491–501. https://doi.org/10.1016/j.omtn.2020.03.011.
13. Shen L, et al. tRNA-Derived small non-coding RNAs as Novel Epigenetic molecules regulating adipogenesis. Biomolecules. 2019;9. https://doi.org/10.3390/biom9070274.
14. Zhang Z, Nie C, Chen Y, Dong Y, Lin T. DNA methylation of CpG sites in the chicken KLF7 promoter and Exon 2 in association with mRNA expression in abdominal adipose tissue and blood metabolic indicators. BMC Genet. 2020;21:120. https://doi.org/10.1186/s12863-020-00923-6.
15. Gong P, et al. Whole-genome bisulfite sequencing of abdominal adipose reveals DNA methylation pattern variations in broiler lines divergently selected for fatness. J Anim Sci. 2021;99. https://doi.org/10.1093/jas/skaa408.
16. Yao Y, et al. METTL3 inhibits BMSC adipogenic differentiation by targeting the JAK1/STAT5/C/EBPbeta pathway via an m(6)A-YTHDF2-dependent manner. FASEB J. 2019;33:7529–44. https://doi.org/10.1096/fj.201802644R.
17. Yi SA, et al. S6K1 phosphorylation of H2B mediates EZH2 trimethylation of H3: a determinant of early adipogenesis. Mol Cell. 2016;62:443–52. https://doi.org/10.1016/j.molcel.2016.03.011.
18. Zhang M, et al. The Landscape of DNA methylation Associated with the Transcriptomic Network of Intramuscular adipocytes generates insight into intramuscular Fat Deposition in Chicken. Front Cell Dev Biol. 2020;8:206. https://doi.org/10.3389/fcell.2020.00206.
19. Song T, et al. Zfp217 mediates m6A mRNA methylation to orchestrate transcriptional and post-transcriptional regulation to promote adipogenic differentiation. Nucleic Acids Res. 2019;47:6130–44. https://doi.org/10.1093/nar/gkz312.
20. Wu R, et al. m6A methylation promotes white-to-beige fat transition by facilitating Hif1a translation. EMBO Rep. 2021;22:e52348. https://doi.org/10.15252/embr.202052348.
21. Guo Z, Shafik AM, Jin P, Wu H. Differential RNA methylation analysis for MeRIP-seq data under general experimental design. Bioinformatics. 2022;38:4705–12. https://doi.org/10.1093/bioinformatics/btac601.
22. Thacker SG, et al. Increased plasma cholesterol esterification by LCAT reduces diet-induced atherosclerosis in SR-BI knockout mice. J Lipid Res. 2015;56:1282–95. https://doi.org/10.1194/jlr.M048629.
23. Hirsch-Reinshagen V, et al. LCAT synthesized by primary astrocytes esterifies cholesterol on glia-derived lipoproteins. J Lipid Res. 2009;50:885–93. https://doi.org/10.1194/jlr.M800584-JLR200.
24. Nesan D, et al. Lecithin:cholesterol acyltransferase (LCAT) Deficiency promotes differentiation of Satellite cells to Brown adipocytes in a cholesterol-dependent manner. J Biol Chem. 2015;290:30514–29. https://doi.org/10.1074/jbc.M115.676056.
25. Dong Z, et al. Loss of LCAT activity in the golden Syrian hamster elicits pro-atherogenic dyslipidemia and enhanced atherosclerosis. Metabolism. 2018;83:245–55. https://doi.org/10.1016/j.metabol.2018.03.003.
26. Lin X, et al. Depleting LCAT aggravates atherosclerosis in LDLR-deficient Hamster with reduced LDL-Cholesterol level. J Adv Res. 2023. https://doi.org/10.1016/j.jare.2023.10.016.
27. Hardfeldt J, et al. Abdominal obesity negatively influences key metrics of reverse cholesterol transport. Biochim Biophys Acta Mol Cell Biol Lipids. 2022;1867:159087. https://doi.org/10.1016/j.bbalip.2021.159087.
28. Qiao M, et al. Molecular characterization, expression profile and association analysis with carcass traits of porcine LCAT gene. Mol Biol Rep. 2010;37:2227–34. https://doi.org/10.1007/s11033-009-9709-x.
29. Chen Y, et al. ALKBH5 suppresses malignancy of hepatocellular carcinoma via m(6)A-guided epigenetic inhibition of LYPD1. Mol Cancer. 2020;19:123. https://doi.org/10.1186/s12943-020-01239-w.
30. Guo X, et al. RNA demethylase ALKBH5 prevents pancreatic cancer progression by posttranscriptional activation of PER1 in an m6A-YTHDF2-dependent manner. Mol Cancer. 2020;19:91. https://doi.org/10.1186/s12943-020-01158-w.
31. Qu J, et al. RNA demethylase ALKBH5 promotes tumorigenesis in multiple myeloma via TRAF1-mediated activation of NF-kappaB and MAPK signaling pathways. Oncogene. 2022;41:400–13. https://doi.org/10.1038/s41388-021-02095-8.

32. Tang C, et al. ALKBH5-dependent m6A demethylation controls splicing and stability of long 3'-UTR mRNAs in male germ cells. Proc Natl Acad Sci U S A. 2018;115:E325–33. https://doi.org/10.1073/pnas.1717794115.

33. Ye G, et al. ALKBH5 facilitates CYP1B1 mRNA degradation via m6A demethylation to alleviate MSC senescence and osteoarthritis progression. Exp Mol Med. 2023;55:1743–56. https://doi.org/10.1038/s12276-023-01059-0.

34. Gao Y, et al. ALKBH5 modulates hematopoietic stem and progenitor cell energy metabolism through m(6)a modification-mediated RNA stability control. Cell Rep. 2023;42:113163. https://doi.org/10.1016/j.celrep.2023.113163.

35. Zhang Q, Cheng B, Jiang H, Zhang H, Li H. N6-methyladenosine demethylase ALKBH5: a novel regulator of proliferation and differentiation of chicken preadipocytes. Acta Biochim Biophys Sin (Shanghai). 2022;54:55–63. https://doi.org/10.3724/abbs.2021007.

36. Ronningen T, et al. m6A regulators in human adipose tissue - Depot-specificity and correlation with obesity. Front Endocrinol (Lausanne). 2021;12:778875. https://doi.org/10.3389/fendo.2021.778875.

37. Wang W, et al. Immortalization of chicken preadipocytes by retroviral transduction of chicken TERT and TR. PLoS ONE. 2017;12:e0177348. https://doi.org/10.1371/journal.pone.0177348.

38. Zhang X, et al. MiR-17-5p and miR-20a promote chicken cell proliferation at least in part by upregulation of c-Myc via MAP3K2 targeting. Sci Rep. 2017;7:15852. https://doi.org/10.1038/s41598-017-15626-9.

39. Zhang X, et al. A transcriptomic and proteomic atlas of obesity and type 2 diabetes in cynomolgus monkeys. Cell Rep. 2023;42:112952. https://doi.org/10.1016/j.celrep.2023.112952.

40. Molinari F, et al. SIRT5 inhibition induces Brown Fat-Like phenotype in 3T3-L1 preadipocytes. Cells. 2021;10. https://doi.org/10.3390/cells10051126.

41. Xiao X, et al. Microglia Sirt6 modulates the transcriptional activity of NRF2 to ameliorate high-fat diet-induced obesity. Mol Med. 2023;29. https://doi.org/10.1186/s10020-023-00676-9.

42. Sugiura K, et al. MuRF1 deficiency prevents age-related fat weight gain, possibly through accumulation of PDK4 in skeletal muscle mitochondria in older mice. J Orthop Res. 2022;40:1026–38. https://doi.org/10.1002/jor.25131.

43. Morrice N, et al. Metformin increases the uptake of glucose into the gut from the circulation in high-fat diet-fed male mice, which is enhanced by a reduction in whole-body Slc2a2 expression. Mol Metab. 2023;77:101807. https://doi.org/10.1016/j.molmet.2023.101807.

44. Cui X, et al. Decreased testosterone levels after caponization leads to abdominal fat deposition in chickens. BMC Genomics. 2018;19:344. https://doi.org/10.1186/s12864-018-4737-3.

45. Wang D, et al. ELOVL gene family plays a virtual role in response to breeding selection and lipid deposition in different tissues in chicken (Gallus gallus). BMC Genomics. 2022;23:705. https://doi.org/10.1186/s12864-022-08932-8.

46. Singh A, et al. Identification of genes affecting milk fat and fatty acid composition in Vrindavani crossbred cattle using 50 K SNP-Chip. Trop Anim Health Prod. 2021;53:347. https://doi.org/10.1007/s11250-021-02795-z.

47. Chen Y, et al. Integrated lipidomics and network pharmacology analysis to reveal the mechanisms of berberine in the treatment of hyperlipidemia. J Transl Med. 2022;20:412. https://doi.org/10.1186/s12967-022-03623-0.

48. Shen Z, et al. FTO inhibits UPR(mt)-induced apoptosis by activating JAK2/STAT3 pathway and reducing m6A level in adipocytes. Apoptosis. 2021;26:474–87. https://doi.org/10.1007/s10495-021-01683-z.

49. Yang Z, Yu GL, Zhu X, Peng TH, Lv YC. Critical roles of FTO-mediated mRNA m6A demethylation in regulating adipogenesis and lipid metabolism: implications in lipid metabolic disorders. Genes Dis. 2022;9:51–61. https://doi.org/10.1016/j.gendis.2021.01.005.

50. Li XC, et al. The m6A demethylase ALKBH5 controls trophoblast invasion at the maternal-fetal interface by regulating the stability of CYR61 mRNA. Theranostics. 2019;9:3853–65. https://doi.org/10.7150/thno.31868.

51. Yu F, et al. Post-translational modification of RNA m6A demethylase ALKBH5 regulates ROS-induced DNA damage response. Nucleic Acids Res. 2021;49:5779–97. https://doi.org/10.1093/nar/gkab415.

52. Cho S et al. mTORC1 promotes cell growth via m(6)A-dependent mRNA degradation. *Mol Cell* 81, 2064–2075 e2068, https://doi.org/10.1016/j.molcel.2021.03.010 (2021).

53. Feng M, et al. YBX1 is required for maintaining myeloid leukemia cell survival by regulating BCL2 stability in an m6A-dependent manner. Blood. 2021;138:71–85. https://doi.org/10.1182/blood.2020009676.

54. Liu L, et al. M(6)a mRNA methylation regulates CTNNB1 to promote the proliferation of hepatoblastoma. Mol Cancer. 2019;18:188. https://doi.org/10.1186/s12943-019-1119-7.

55. Zhao X, et al. FTO-dependent demethylation of N6-methyladenosine regulates mRNA splicing and is required for adipogenesis. Cell Res. 2014;24:1403–19. https://doi.org/10.1038/cr.2014.151.

56. Zhang K, et al. N(6)-methyladenosine-mediated LDHA induction potentiates chemoresistance of colorectal cancer cells through metabolic reprogramming. Theranostics. 2022;12:4802–17. https://doi.org/10.7150/thno.73746.

57. Wang L, et al. NADP modulates RNA m(6)a methylation and adipogenesis via enhancing FTO activity. Nat Chem Biol. 2020;16:1394–402. https://doi.org/10.1038/s41589-020-0601-2.

58. Chen J, et al. ALKBH5 enhances lipid metabolism reprogramming by increasing stability of FABP5 to promote pancreatic neuroendocrine neoplasms progression in an m6A-IGF2BP2-dependent manner. J Transl Med. 2023;21:741. https://doi.org/10.1186/s12967-023-04578-6.

59. Chen J, et al. Inhibition of ALKBH5 attenuates I/R-induced renal injury in male mice by promoting Ccl28 m6A modification and increasing Treg recruitment. Nat Commun. 2023;14:1161. https://doi.org/10.1038/s41467-023-36747-y.

60. Sasaki M, et al. Novel LCAT (lecithin:cholesterol acyltransferase) activator DS-8190a prevents the progression of Plaque Accumulation in Atherosclerosis models. Arterioscler Thromb Vasc Biol. 2021;41:360–76. https://doi.org/10.1161/ATVBAHA.120.314516.

61. Li L, et al. Lecithin cholesterol acyltransferase null mice are protected from diet-induced obesity and insulin resistance in a gender-specific manner through multiple pathways. J Biol Chem. 2011;286:17809–20. https://doi.org/10.1074/jbc.M110.180893.

62. Xepapadaki E, et al. Impact of apolipoprotein A1- or lecithin:cholesterol acyltransferase-deficiency on white adipose tissue metabolic activity and glucose homeostasis in mice. Biochim Biophys Acta Mol Basis Dis. 2019;1865:1351–60. https://doi.org/10.1016/j.bbadis.2019.02.003.

63. Wu W, et al. Untargeted metabolomic and lipid metabolism-related gene expression analyses of the effects and mechanism of aged Liupao tea treatment in HFD-induced obese mice. RSC Adv. 2021;11:23791–800. https://doi.org/10.1039/d1ra04438a.

Publisher's Note